Article

Fabrication of Mesoporous SiO_2@$CaSiO_3$ Hollow Spheres as Carriers for pH-sensitive Drug Delivery

YUAN Mingwei, SHI Shunli, LUO Yanping, YU Ying, WANG Shuhua✉ and CHEN Chao✉

Received June 18, 2021
Accepted August 18, 2021

Hollow mesoporous silica(HM-SiO_2) was prepared by the improved stober method. On this basis, HM-SiO_2 was dispersed in an alkaline solution for surface etching. Meanwhile, calcium source was introduced to combine with SiO_3^{2-} on the surface to form a $CaSiO_3$ shell layer and an unprecedent SiO_2@$CaSiO_3$ sphere with a hollow double-shell structure was obtained. The as-synthesized SiO_2@$CaSiO_3$ was characterized by X-ray diffraction(XRD), scanning electron microscopy(SEM), transmission electron microscopy(TEM), N_2-BET, IR and UV-Vis techniques, and its sustained release capacity of doxorubicin(DOX) loading was investigated. The drug loading capacity can be achieved to 0.692 mg DOX/mg SiO_2@$CaSiO_3$, exhibiting pH-responsivity under low pH conditions.

Keywords Hollow nano-sphere; SiO_2@$CaSiO_3$; Drug delivery; pH-Sensitive

1 Introduction

In recent years, the clinical use of excessive drugs has been greatly limited due to the physical impairment caused by drug release and the deterioration of drug properties by repeated administration[1]. Hence, the study of drug loading and sustained release has attracted the attention of researchers[2]. For a drug carrier, in addition to its composition, the microstructure design with a high specific surface area acts as the key factor in its drug delivery ability and release behavior[3].

Many functional nanomaterials, such as gold nanoparticles, quantum dots, carbon nanotubes, magnetic nanoparticles, liposomes and silicon nanoparticles have been used for potential applications on the development of drug delivery[4—7]. Among these nanoparticles, nano-SiO_2 is an amorphous inorganic non-metallic material, non-toxic, tasteless and pollution-free[8]. The material enjoys a stable network quasi particle structure, a small particle size, a large pore volume, a large specific surface area, and a good adsorption effect[9]. Whether SiO_2 is monodisperse silica, mesoporous silica or hollow silica, it has a wide range of applications in the fields of optics, photonic crystals, catalysis, drug delivery carrier and so on[10]. Therefore, it has attracted mounting attention from researchers. Addtionally, inorganic bioceramics, such as tricalcium phosphate, bioactive glass, hydroxyapatite[$Ca_{10}(PO_4)_6(OH)_2$], $CaSiO_3$ and other materials, which are widely used in clinical practice, have great application potential in bone tissue engineering, drug delivery and diagnosis due to their similar biological structure to human bones and good cell compatibility[11]. In particular, owing to its good biological activity, biodegradability and high drug loading capacities(DLCs), calcium silicate has been considered as an excellent candidate material for bone regeneration and drug carrier in recent years.

Nanoscience and nanotechnology researches are gradually shifting from the individual component to hybridnanostructured materials, especially the complex nanocomposites. In general, the nanocomposites show novel properties and multifunctions[12,13]. The hollow-coregulate-shell nanocomposites(HCMSN), which contain a hollow core and multi-shells with different components have attracted much attention in the past years[14,15]. Zhu *et al*.[16] synthesized the HCMSN with a Fe_3O_4@SiO_2 hollow mesoporous spheres as carriers for drug delivery. Wu *et al*.[17] prepared hierarchically nanostructured mesoporous spheres of calcium silicate hydrate in surfactant-free sonochemical synthesis for drug-delivery. Prasanna *et al*.[18] prepared multifunctional ZnO/SiO_2 core/shell nanoparticles for bioimaging and drug delivery application.

It can be seen from the above reviews that hollow SiO_2 and $CaSiO_3$ are the important inorganic biomaterials. The hollow structure makes the material high permeable and low dense, and its large cavity is more conducive to the loading of the drug[19]. $CaSiO_3$ has good biological activity and biodegradability, which provides a broad prospect for its application in bone repair and drug delivery[20,21]. Therefore, hollow $CaSiO_3$-coated silica nanocomposites would be ideal reagents for medical diagnosis and treatment. However, the typical lamellar structure of $CaSiO_3$ prepared by traditional hydrothermal methods makes it difficult to uniformly grow on the surface of hollow SiO_2. Therefore, the development of

✉ WANG Shuhua
shwang@ncu.edu.cn
✉ CHEN Chao
chaochen@ncu.edu.cn
Key Laboratory of Jiangxi Province for Environment and Energy Catalysis, College of Chemistry, Nanchang University, Nanchang 330031, P. R. China

https://doi.org/10.1007/s40242-021-1248-6

SiO_2@$CaSiO_3$ nanocomposites with a double-shell hollow structure is meaningful although challenging. Herein, on the basis of hollow mesoporous silica with a regular morphology, we have employed *in-situ* surface etching method to grow calcium silicate on the SiO_2 shell. The as-synthesized hollow SiO_2@$CaSiO_3$ maintains the original mesoporous properties of SiO_2, with a specific surface area of up to 1123 m^2/g. The drug can be loaded on it up to 0.692 mg DOX/mg SiO_2@$CaSiO_3$, and has pH response under low pH conditions.

2 Experimental

2.1 Materials

Tetraethyl orthosilicate(TEOS), $Si(OC_2H_5)_4$, calcium nitrate tetrahydrate[$Ca(NO_3)_2{\cdot}4H_2O$], sodium hydroxide(NaOH) and anhydrous ethanol were all purchased from Sinopharm Chemical Reagent Co., Ltd. Phosphate buffer saline(PBS) and cetyltrimethylammonium bromide(CTAB, $C_{19}H_{42}BrN$) were received from Innochem Chemical Reagents Co., Ltd. Ammonium hydroxide(NH_4OH, 30%, mass fraction) was obtained from Energy Chemical Co., Ltd. Doxorubicin hydrochloride(DOX, >99%) was provided by Aladdin Reagent Co., Ltd. All the reagents were used without further purification.

2.2 Preparation of Drug Carrier

2.2.1 Synthesis of HM-SiO_2

According to the literature[22], HM-SiO_2 was prepared by the improved stober method. Ethanol(60 mL) and 100 mL of water were mixed evenly, and 300 mg of CTAB was dispersed in the mixed solvent, followed by ultrasonic dispersion for 10 min. Drop 2 mL of ammonia water with a mass concentration of 30%, and drop 2 mL of TEOS under rapid stirring. The resulting mixed solution was subjected to a water bath reaction at 35 °C for 24 h, during which rapid stirring was carried out to prevent agglomeration. At the end of the reaction, the M-SiO_2 was centrifugally washed repeatedly with water and ethanol until pH was neutral. The obtained M-SiO_2 was transferred to a 500 mL round-bottom flask, and a large amount of deionized water was added. The flask was stirred and refluxed at 70 °C for 20 h, then centrifugally washed with water and ethanol twice respectively, and finally dried in a vacuum drying oven at 60 °C for 24 h to obtain HM-SiO_2. In order to remove the residual CTAB in HM-SiO_2 channels, HM-SiO_2 was dispersed into 150 mL of anhydrous ethanol, and 250 μL of hydrochloric acid was added. After being refluxed at 70 °C for 10 h, HM-SiO_2 was centrifugally washed with water and ethanol twice respectively, and then placed in a vacuum drying oven for drying at 60 °C for 24 h.

2.2.2 Synthesis of Hollow SiO_2@$CaSiO_3$

Take 200 mg of HM-SiO_2 dispersed in 150 mL of deionized water, 50 mg of CTAB was added under stirring condition, and stirred at 25 °C for 30 min at a constant speed. Sodium hydroxide solution(1 mol/L) was added for etching, and pH was adjusted to 12. Then, 80 mg of $Ca(NO_3)_2{\cdot}4H_2O$ was dispersed in 5 mL of deionized water and dropped into the reaction solution within 15 min. The reaction was evenly stirred at 95 °C for 3 h. After the reaction, each of them was centrifugally washed with water and ethanol twice, and then transferred to a vacuum drying oven for drying at 60 °C for 24 h to obtain SiO_2@$CaSiO_3$ hollow nano-spheres.

2.3 Material Characterization

Powder X-ray diffraction(PXRD) patterns were recorded by using a RigakuXRD-6000 diffractometer(operating at 40 kV and 30 mA) with Cu *Kα* radiation. Scanning electron microscopy(SEM) images were obtained on a field emission scanning electron microscope JSM 6701F. Transmission electron microscopy(TEM) and high-resolution TEM(HRTEM) images were acquired by a JEOL JEM-2010F. Nitrogen adsorption isotherm was measured on an Autosorb iQ2 analyzer (Quantachrome). The surface area was calculated by the multi-point BET method and the pore volume and pore diameter by the BJH formula. FTIR spectra were obtained in the range of 4000—400 cm^{-1} using a Nicolet iS10 with a resolution of 0.3 cm^{-1}. The concentration of DOX was determined by UV-Vis spectroscopic analysis.

2.4 *In vitro* Loading and Release of DOX

Six portions of 40 mg of SiO_2@$CaSiO_3$ hollow nano-spheres were placed in 40 mL of DOX solution with concentrations of 0.05, 0.1, 0.2, 0.5, 1.0, and 1.2 mg/mL, respectively, and mixed at a constant speed for 24 h without light. The SiO_2@$CaSiO_3$ hollow nano-spheres loaded with DOX were obtained and centrifuged at an overspeed centrifuge(8000 r/min). Supernatant(3 mL) was taken each time, and 3 mL of deionized water was added. After three times centrifugation, the ultraviolet absorbance of the supernatant at the wavelength of 480 nm was measured to determine the drug loading and encapsulation rate at different initial concentrations. Two copies of 20 mg of DOX loaded SiO_2@$CaSiO_3$ hollow nano-spheres were put into two dialysis bags with the interception molecular weight of 3500[23]. Then they were placed in 60 mL of PBS solution(pH 7.4 and 4.5 adjusted by 0.5% HCl) and magnetic stirred in a 37 °C water bath for *in vitro* sustained release experiment. At 1, 2, 4, 6, 12, 24, 36, 48, 60, 72, 84, 96,

https://doi.org/10.1007/s40242-021-1248-6

108 and 120 h, 3 mL of sustaining-release solution was taken out, and then 3 mL of PBS solution with the same pH was added. Ultraviolet spectrophotometer was used to measure the ultraviolet absorbance of the sustained-release solution at the wavelength of 480 nm at each time point, and the DOX concentration in the supernatant at this time was obtained according to the DOX standard curve.

3 Results and Discussion

3.1 Double-shell SiO_2@$CaSiO_3$ Hollow Sphere Fabrication

The preparation process of SiO_2@$CaSiO_3$ is shown in Fig.1. First of all, M-SiO_2 was prepared by the improved stober method. Then, the internal SiO_2 was dissolved preferentially under the condition of reflux in water and HM-SiO_2 was obtained, due to the internal instability of the silicon sphere compared with the external one, which was similar to the Oswald ripening process. The residual CTAB in the pore was removed by reflux in acidic ethanol solution to further expand the specific surface area of the material. A calcium source was introduced under alkaline conditions, and a layer of $CaSiO_3$ shell layer was grown on the surface while HM-SiO_2 was etched. Finally, hollow SiO_2@$CaSiO_3$ was obtained by centrifugation.

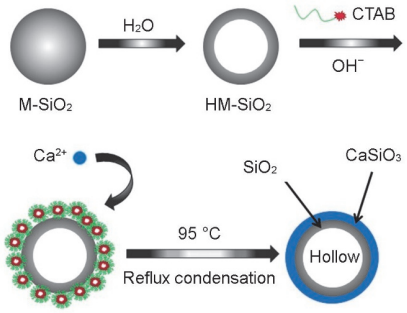

Fig.1 Schematic diagram of the preparation procedure for double-shell SiO_2@$CaSiO_3$ hollow sphere

3.2 Structure Characterization

The crystal structure of the synthesized samples was determined by PXRD analysis. As shown in Fig.2(A), M-SiO_2 and HM-SiO_2 both showed the broad peak characteristic of the amorphous materials[24]. After the growth of the $CaSiO_3$ shell, all the diffraction peaks were relatively dispersed except for the strong diffraction peak at 2θ=29°, indicating that the crystallinity of the sample was low and the sample belonged to amorphous material. The diffraction peak at 29° was basically consistent with the XRD characteristic peaks of

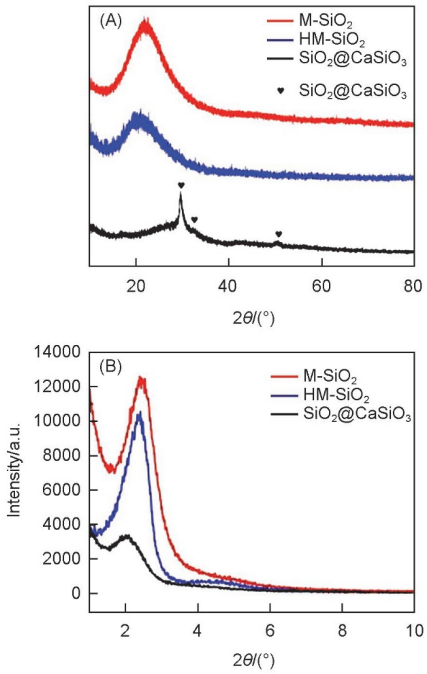

Fig.2 PXRD patterns(A) and small angle X-ray diffraction patterns(B) of M-SiO_2, HM-SiO_2 and hollow SiO_2@$CaSiO_3$

$CaSiO_3$ hydrate reported by Wu *et al.*[25], revealing the formation of $CaSiO_3$ shell. In order to study the mesoporous properties of the material, small angle X-ray diffraction test was carried out on HM-SiO_2. As shown in Fig.2(B), the small angle X-ray diffraction of M-SiO_2, HM-SiO_2 and SiO_2@$CaSiO_3$ demonstrated that ordered mesopores existed in the prepared material[26]. The crystallinity of HM-SiO_2 has been damaged to a certain extent after reflow in the water, leading to a slight reduction in the intensity of the small-angle X-ray diffraction peak. Compared with silica, the strength of SiO_2@$CaSiO_3$ obviously weakened after the growth of the calcium silicate shell, as its layer is wrapped, and the ordered mesopores have a greater impact, so the intensity of the X-ray small-angle diffraction peak drops significantly.

The morphology and structure of M-SiO_2, HM-SiO_2 and SiO_2@$CaSiO_3$ were analyzed by SEM and TEM. As shown in Fig.3(A), M-SiO_2 was spherical with a regular morphology and a uniformly dispersed particle size around 400 nm. HM-SiO_2 obtained after cavity dissolution is manifested in Fig.3(B). Its surface was still smooth but large cavity could be seen from TEM images, indicating the formation of the hollow structure. After the outer layer of $CaSiO_3$ growing, the surface of the silicon sphere became rough, and the size was slightly increased to about 500 nm. As shown in Fig.3(C), the synthetic SiO_2@$CaSiO_3$ was characterized by elemental mapping test for element distribution analysis. The element distribution of Ca, O and Si in hollow SiO_2@$CaSiO_3$ is demonstrated in Fig.3(D). It could be seen that the inner ring SiO_2 had a bright aperture,

https://doi.org/10.1007/s40242-021-1248-6

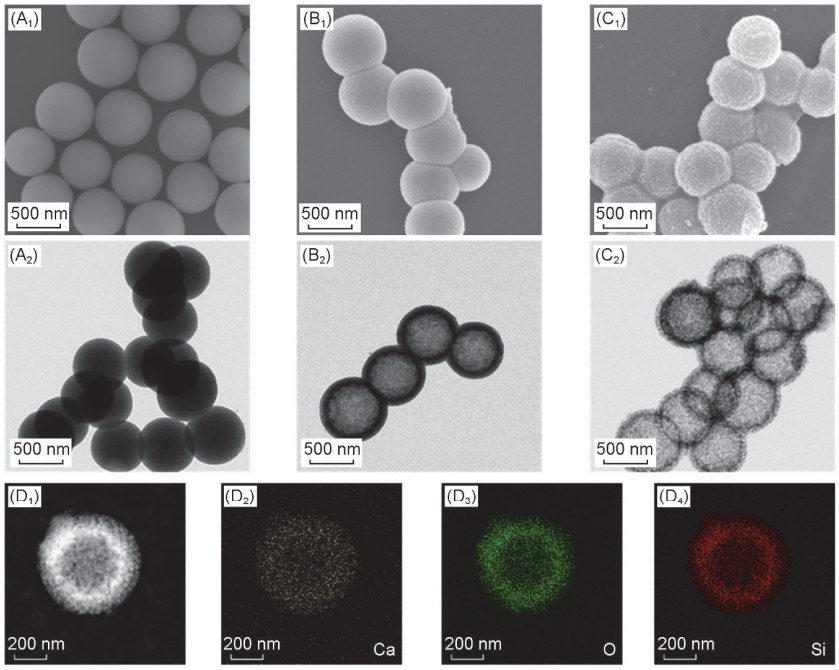

Fig.3 SEM(A_1—C_1), and TEM(A_2—C_2) images for M-SiO_2(A_1, A_2), HM-SiO_2(B_1, B_2) and hollow SiO_2@$CaSiO_3$(C_1, C_2), respectively, and the EDS elemental mappings of void SiO_2@$CaSiO_3$ nanosphere(D_1—D_4)

and Ca element was uniformly distributed throughout the surface of the sphere. The distribution of O and Si elements presented a uniform spherical shape, which was consistent with the distribution size of Ca elements. It proved that the surface of the material have grown uniformly with $CaSiO_3$ shells. Meanwhile, the content of O and Si elements in the inner layer was significantly higher than that in other parts, indicating that part of the HM-SiO_2 shells were retained in the inner layer. This information was consistent with the previous SEM and TEM.

Since the large specific surface area and the ordered mesoporous are more conducive to the drug loading of the material, the N_2 adsorption/desorption isotherms of the sample were conducted. The pore structure, specific surface area and other properties of the materials were analyzed. As depicted in Fig.4, HM-SiO_2 and SiO_2@$CaSiO_3$ had multi-level

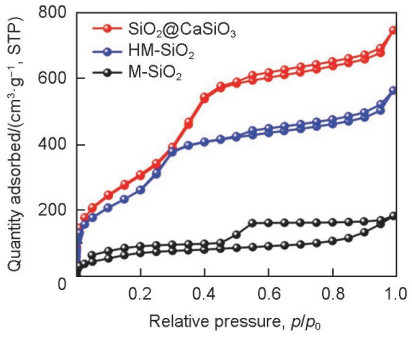

Fig.4 N_2 adsorption-desorption isotherms of M-SiO_2, HM-SiO_2 and hollow SiO_2@$CaSiO_3$

channels and hysteresis loops. Compared with M-SiO_2, a small number of micropores appeared in the samples after cavitation dissolution, as a small number of mesopores were blocked during the process of dissolution from the inside of the silicon sphere to the outside during cavitation dissolution in the deionized water. The specific surface area, pore volume and pore diameter distribution data of the samples calculated by BJH method are illustrated in Table 1. The specific surface area of the samples after cavitation dissolution was greatly improved compared with that of M-SiO_2, while the pore diameter changed little. Removal of the pore-forming agent CTAB in acidic ethanol solution resulted in a significant increase in the specific surface area compared with M-SiO_2. After coating calcium silicate shell, the samples still had mesoporous properties. Therefore, our synthesized SiO_2@$CaSiO_3$ mesoporous hollow nano-spheres had a large specific surface area and ordered mesoporous structure, which were beneficial to drug loading.

Fig.5 displays the FTIR spectra diagram of SiO_2@$CaSiO_3$ prepared before and after drug loading. The absorption peaks at 1091 cm^{-1} were the asymmetric stretching vibration and the symmetric stretching vibration of Si—O—Si bond. The curved

Table 1 Structural properties of M-SiO_2, HM-SiO_2 and hollow SiO_2@$CaSiO_3$

Sample	S_{BET}/($m^2 \cdot g^{-1}$)	V_P/($cm^3 \cdot g^{-1}$)	D_P/nm
M-SiO_2	252	0.243	4.15
HM-SiO_2	1139	0.745	2.77
SiO_2@$CaSiO_3$	1123	0.993	3.17

https://doi.org/10.1007/s40242-021-1248-6

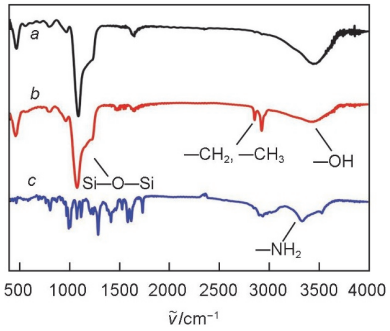

Fig.5 FTIR spectra of SiO_2@$CaSiO_3$(*a*), DOX/SiO_2@$CaSiO_3$(*b*) and DOX(*c*)

Si—O—Si mode produced the adsorption band at 463 cm^{-1}, while the curved 1637 cm^{-1} was the vibration absorption peak of H—OH, which may be caused by the water absorption of silicon in the air. The asymmetric tensile vibration of structure water —OH was 3477 cm^{-1}. The extremely weak absorption peak near 967 cm^{-1} was the bending vibration absorption peak of Si—OH. In general, the dehydration of Si—OH turned into Si—O—Si, so the absorption peak of Si—OH could hardly be seen in the infrared spectrum[26,27]. After loading DOX, the characteristic peaks of —CH_3 and —CH_2 of DOX appeared in the FTIR(Fig.5 curve *b*), and the stretching vibration peak of —OH on the surface was weakened, indicating that the drug was successfully loaded on the hollow nano-sphere SiO_2@$CaSiO_3$.

3.3 Drug Loading and Sustained-release Properties

DOX, as a popular anticancer drug, has been widely used in the chemotherapy treatment of various cancers, and has achieved excellent clinical effects. In order to determine the maximum drug loading of the prepared SiO_2@$CaSiO_3$ hollow nano-spheres, we soaked the carrier with the same mass in DOX solution with the concentrations of 0.05, 0.1, 0.2, 0.5, 1.0, and 1.2 mg/mL, respectively. The corresponding ratios of *m*(DOX) to *m*(SiO_2@$CaSiO_3$) were 0.05, 0.1, 0.2, 0.5, 1.0 and 1.2, respectively. The results are listed in Table 2. In the DOX solution with low concentration, the loading efficiency(LE) of SiO_2@$CaSiO_3$ hollow nano-spheres for DOX was as high as 95.6%. With the increase of concentration, the LE value gradually decreased to reach the carrier saturation adsorption capacity, and the drug loading capacity(DLC) value reached 0.692 mg DOX/mg SiO_2@$CaSiO_3$. Compared with similar silicon materials in the literature[27], Lin *et al.*[28] synthesized nano SiO_2 to load DOX, and its DLCs and LE reached 42.6% and 85.2%, respectively. The reason is that the material's large specific surface area and ordered mesoporous properties are more conducive to drug loading.

Table 2 Drug loading capacity of hollow SiO_2@$CaSiO_3$*

m(DOX)/ *m*(SiO_2@$CaSiO_3$)	DLC/(mg DOX·mg^{-1} SiO_2@$CaSiO_3$)	Loading efficiency(%)
0.05	0.048	95.6
0.1	0.088	87.5
0.2	0.159	79.5
0.5	0.375	75.0
1.0	0.692	69.2
1.2	0.688	57.3

* Drug loading capacity=*m*(drug)/*m*(SiO_2@$CaSiO_3$). Loading efficiency: the ratio of loaded amount of drug to the initial amount of drug.

In order to study the slow-release ability and pH response ability of the material, we put the hollow nano-spheres with the largest loading capacity and *m*(DOX)/*m*(SiO_2@$CaSiO_3$) of 1 into dialysis bags with the interception molecular weight of 3500, and soaked them in pH of 7.4 and 4.5, respectively. In the PBS buffer solution at 37 °C, the response of the carrier to the slow release of the drug in neutral and acidic environment was simulated. As shown in Fig.6, the sustained release time of the carrier was as long as 120 h under different pH conditions, exhibiting the characteristics of long-term administration and slow release. Under neutral condition, the release amount was only 52%, while the release rate was significantly accelerated under pH=4.5. We believed that the —NH_2 groups of DOX formed hydrogen bonded with the Si—OH groups on the surface of SiO_2@$CaSiO_3$, and the the —NH_2 groups on the surface of the DOX were protonated and loaded on the surface of the carrier through electrostatic adsorption. In the pH=4.5 environment, the calcium silicate shell was destroyed. At the same time, the interaction between the drug molecule and carrier was weakened. DOX escaped from DOX-loaded SiO_2@$CaSiO_3$ and dissolved quickly in acidic environment, leading to a higher release rate at the same time. This characteristic of pH-responsive drug release has important implications for drug development.

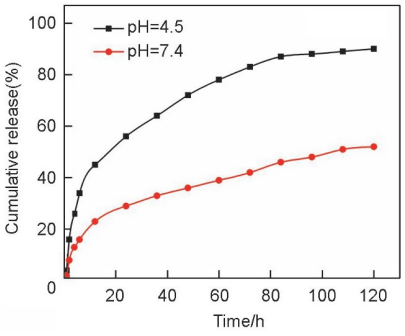

Fig.6 Release profile of DOX from DOX-loaded SiO_2@$CaSiO_3$ hollow mesoporous spheres in PBS at 37 °C in different pH media

4 Conclusions

In summary, we successfully synthesized hollow mesoporous

https://doi.org/10.1007/s40242-021-1248-6

SiO_2@$CaSiO_3$ nano-spheres and applied them to the loading and sustained-release of DOX model drugs. The material has regular morphology and specific surface area of up to 1123 m^2/g, It can load up to 0.692 mg DOX/mg SiO_2@$CaSiO_3$ and has the function of pH response, which is beneficial to avoiding the rapid release of drugs in neutral blood system, and promoting the release of drugs in acidic tumor sites or cells. Therefore, as an excellent osteogenic material, the as-synthesized SiO_2@$CaSiO_3$ has good compatibility with the human body, non-toxic and harmless, and its special mesoporous structure makes this material greatly applied in the fields of catalysis, chromatographic analysis and biosensing.

Acknowledgements

This work was supported by the National Natural Science Foundation of China (No.21961021) and the Natural Science Foundation of Jiangxi Province, China (No.20202ACB203001).

Conflicts of Interest

The authors declare no conflicts of interest.

References

[1] Torchilin V. P., *Nat. Rev. Drug Discov.,* **2014**, *13*(11), 813
[2] Blanco E., Shen H., Ferrari M., *Nat. Biotechnol.,* **2015**, *33*(9), 941
[3] Wang S., *Micropor. Mesopor. Mat.,* **2009**, *117*(1/2), 1
[4] Cheng L., Wang C., Feng L., Yang K., Liu Z., *Chem. Rev.,* **2014**, *114*(21), 10869
[5] Suk J. S., Xu Q., Kim N., Hanes J., Ensign L. M., *Adv. Drug. Deliv. Rev.,* **2016**, *99*(Pt. A), 28
[6] Karimi M., Ghasemi A., SahandiZangabad P., Rahighi R., MoosaviBasri S. M., Mirshekari H., Amiri M., ShafaeiPishabad Z., Aslani A., Bozorgomid M., Ghosh D., Beyzavi A., Vaseghi A., Aref A. R., Haghani L., Bahrami S., Hamblin M. R., *Chem. Soc. Rev.,* **2016**, *45*(5), 1457
[7] Hou X., Zhao C., Tian Y., Dou S., Zhang X., Zhao J., *Chem. Res. Chinese Universities,* **2016**, *32*(6), 889
[8] Tu X., Wang L., Cao Y., Ma Y., Shen H., Zhang M., Zhang Z., *Carbon,* **2016**, *97*, 35
[9] Wu P., Zhou D., Huang Y., Li J., *Chem. Res. Chinese Universities,* **2018**, *34*(4), 676
[10] Rong Z., Sun W., Xiao H., Jiang G., *Cement Concrete Comp.,* **2015**, *56*, 25
[11] Islam M. S., Choi H. N., Choi W. S., Lee H.-J., *J. Mater. Chem. B,* **2015**, *3*(6), 1001
[12] Lu B.-Q., Zhu Y.-J., Cheng G.-F., Ruan Y.-J., *Mater. Lett.,* **2013**, *104*, 53
[13] Chen Z., Yan X., Li M., Wang S., Chen C., *Inorg. Chem.,* **2021**, *60*(7), 4362
[14] Li C., Wang J. C., Wang Y. G., Gao H. L., Wei G., Huang Y. Z., Yu H. J., Gan Y., Wang Y. J., Mei L., Chen H. B., Hu H. Y., Zhang Z. P., Jin Y. G., *Acta Pharm. Sin. B,* **2019**, *9*(6), 1145
[15] Fenton O. S., Olafson K. N., Pillai P. S., Mitchell M. J., Langer R., *Adv. Mater.,* **2018**, *30*(29), 1
[16] Zhu Y. F., Ikoma T., Hanagata N., Kaskel S., *Small*, **2010**, *6*(3), 471
[17] Wu J., Zhu Y.-J., Cao S.-W., Chen F., *Adv. Mater.*, **2010**, *22*(6), 749
[18] Prasanna A. P. S., Venkataprasanna K. S., Pannerselvam B., Asokan V., Jeniffer R. S., Venkatasubbu G. D., *J. Fluoresc.,* **2020**, *30*(5), 1075
[19] Wu C., Chang J., Fan W., *Journal of Materials Chemistry*, **2012**, *22*(33), 16801
[20] Zhu Y.-J., Guo X.-X., Sham T.-K., *Expert Opin. Drug Del.,* **2017**, *14*(2), 215
[21] Ge R., Xun C., Yang J., Jia W., Li Y., *Biomed. Mater.,* **2019**, *14*(6), 065013
[22] Teng Z., Su X., Zheng Y., Sun J., Chen G., Tian C., Wang J., Li H., Zhao Y., Lu G., *Chem. Mater.,* **2012**, *25*(1), 98
[23] Dou Y., Guo J., Chen Y., Han S., Xu X., Shi Q., Jia Y., Liu Y., Deng Y., Wang R., Li X., Zhang J., *J. Control. Release.,* **2016**, *235*, 48
[24] Vallet-Regi M., Colilla M., Izquierdo-Barba I., Manzano M., *Molecules,* **2018**, *23*(1), 19
[25] Wu J., Zhu Y.-J., Chen F., *Small,* **2013**, *9*(17), 2911
[26] Christoforidou T., Giasafaki D., Andriotis E. G., Bouropoulos N., Theodoroula N. F., Vizirianakis I. S., Steriotis T., Charalambopoulou G., Fatouros D. G., *Int. J. Mol. Sci.,* **2021**, *22*(4), 1896
[27] Liu L., Liu J., Zhao L., Yang Z., Lv C., Xue J., Tang A., *Environ. Sci. Pollut. Res.,* **2019**, *26*(9), 8721
[28] Lin Z. T., Wu Y. B., Bi Y. G., *J. Nanopart. Res.,* **2018**, *20*(11), 13